ICEMG 2023-XXXXX

Design of a fractional slot concentrated winding double-speed AFPM motor

Reza Mirzahosseini[1], Elham Rahimi Namaghi[2]
[1]Faculty of Electrical Engineering, Shahrood University of Technology, Shahrood,
E-mail: reza.mirzahosseini78@gmail.com
[2]Faculty of Electrical and Computer Engineering, Semnan University, Semnan,
E-mail: elhamrahimi_1367@yahoo.com

Abstract
In this paper, a new topology of fractional slot concentrated winding double rotor axial flux permanent magnet synchronous motor (FSCW-DRAFPMSM) is introduced. The desired structure consists of a non-slotted stator core and two rotor discs. The pole number of the two rotors is different and these two rotors rotate at different speeds in opposite directions. A sample motor with output power of 200 Watts is designed with the proposed structure. The two rotors of this sample motor rotate with speeds of 600 and 428 rpm. The Finite Element Method (FEM) is employed to evaluate the performance of the proposed structure. Some performance characteristics of the case study machine, such as the Back EMF, input power, and electromagnetic torques of two rotors, … are presented to confirm the correctness of the operation of the proposed structure. In addition, the shifting technique is used to improve the Back EMF waveform of the machine.

Keywords: Axial Flux Permanent Magnet (AFPM), Counter-rotating, Dual-rotor, Fractional slot concentrated winding.

Introduction

Electrical motors are widely used in many industrial applications such as electric vehicles, fans, elevators, etc. [1,2]. Distributed winding and concentrated winding are two common types of windings that have been used in permanent magnet (PM) machines. High-power density, high efficiency, short-end turn, slow cogging torque, and high slot fill factor are advantages of concentrated winding in comparison to distributed winding [3-5]. Despite these advantages, Concentrated windings produce a non-sinusoidal magnetomotive force (MMF) distribution along the air gap. Hence, the air-gap flux density has many low and high-order spatial harmonics. In PM machines, these harmonics induce large rotor magnet losses. In asynchronous machines, they induce high rotor bar losses as well as various parasitic torque components that degrade the machine's average torque. In synchronous reluctance machines, they lead to high torque ripples. Moreover, spatial harmonics cause local saturation, additional stator and rotor losses, acoustic noise, and vibration. Several papers have been studied on concentrated windings. In [7], the design and analysis of fractional slot concentrated winding (FSCW) PM machines have been studied. Also, commercial applications of this structure have been presented. In [8], an overview of recent research in the field of FSCW machine optimization has been presented. The general formulation of the winding factor for the FSCW has been performed. Also, the winding factor is redefined for stator windings without any information on the number of poles [9]. In [10], a generator with FSCW for use in low-voltage applications in distributed generation has been proposed. The generator is designed based on (FE) analysis. In [11], a permanent magnet (PM) vernier motor with FSCW has been introduced. The induced voltage is analyzed through FE simulations and compared with their analytical calculation results. A five-phase FSCW has been presented. One of the advantages of this structure, in addition to having the advantages of the conventional FSCW, is weak space harmonics of magnetomotive force (MMF). In desired structure, a stator shift technique combined with a star/pentagon winding connection has been used. Compared to the conventional model, the first harmonic of MMF in the new winding is eliminated. Moreover, the non-overlapping characteristics of FSCW are kept. The winding factor of new winding is improved, and the total harmonic distortion (THD) of MMF is reduced by 2.1% [12]. In [13], the effect of the number of winding layers on the performance of FSCW interior permanent magnet machines has been evaluated. Investigation of the results shows that the high number of layers can have a significant improvement in efficiency and torque density. In [14], by both methods of the nonlinear magnetic circuit and FEM, the mechanism of reducing magnetic saturation by the FSCW technique is investigated. A synchronous reluctance machine with FSCW has been introduced. To eliminate the unwanted MMF harmonics, stator shifting has been used. Also, the comprehensive comparisons for the case study machine equipped with FSCW and also distributed winding are presented [15].

Our studies show that the researchers in the previous papers tried to mitigate the harmonics of MMF. However, these harmonics can be useful for designing a machine with a new structure. In the present paper, a topology for a non-slotted double rotor AFPM machine is introduced that operates based on harmonics components of MMF. This proposed structure has two rotor discs that rotate in opposite directions.

Topology of the proposed machine

Generally, decreasing the harmonic components of the stator MMF and increasing the first harmonic order are the main objectives of proposing a new winding arrangement. The fifth and seventh harmonics of the MMF are often the dominant harmonics component of the MMF. These two MMF harmonics rotate in opposite directions. However, if the machine is designed in a way that the fifth and seventh harmonics have

significant amplitudes, we can use these two harmonics to have a machine with two different rotating directions. On the other hand, the pole number of an electrical machine must be an even number. Therefore, it is possible to design a machine with two rotors and one stator disc in a way that one of the rotors has 10 poles while the other one has 14 poles. One rotor disc rotates clockwise while the other rotor rotates counterclockwise, independently. The FSCW has significant harmonic components compared to distributed winding. Therefore, the FSCW is a good choice to have a machine with high amplitudes of fifth and seventh harmonics. The pole arc to pole pitch α_i has a significant influence on the amplitudes of the fifth and seventh harmonics of MMF. By varying the value of α_i can achieve a sinusoidal or trapezoidal Back EMF. This parameter can increase the amplitudes of the fifth and seventh harmonics of the Back EMF. The double-rotor Axial flux permanent magnet (AFPM) machine is a good candidate to have a machine with two opposite directions of rotation, simultaneously. The machine topology is shown in Figure 1. The machine structure includes a toroidal wounded stator in the middle and two independent rotors on both sides. The stator core is fabricated from high silicon–iron alloys while low-carbon steel is employed for rotor cores. Each rotor disc carries a certain number of PMs placed on the inner surface of the rotor core. The single-layer FSCW has been used in the structure of the proposed topology. The 2-D schematic of the winding arrangement is shown in Figure 2. In this figure, the direction of the current in each coil is indicated by a dot (.) and a cross (×).

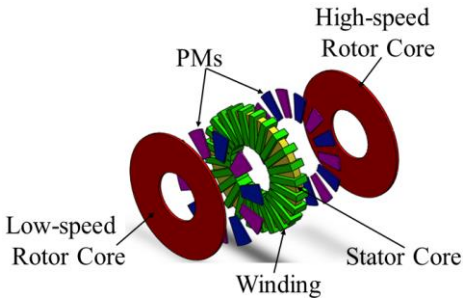

Figure 1. The structure of the machine.

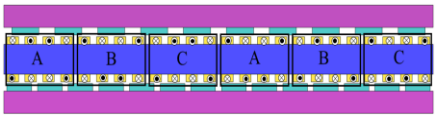

Figure 2. The winding arrangement of the machine.

Evaluating the operation of the machine

A sample machine with the specifications given in Table 1 has been designed. The material of the machine's parts is presented in Table 2. To evaluate the performance of the machine, several simulations have been implemented using FEM. As is clear, the structure of the machine is symmetrical. Therefore, for reducing the volume of calculations and saving program running time, the 2-D structure of the machine in average diameter is simulated in FE software. The major flux density in the machine is due to the magnetic fluxes of PMs. The magnetic fluxes and induced voltage in the armature windings due to each rotor PMs are obtained, easily. For this purpose, by applying the air to the PMs of each rotor, the magnetic fluxes and induced voltage due to the other rotor PMs are attained. In Figure 3, the magnetic flux distribution due to the high-speed rotor PMs at no-load conditions is shown. In Figure 4, the induced voltage in the stator windings due to the high-speed rotor PMs is illustrated. A similar procedure has been employed to obtain the flux density distribution and induced voltages due to the low-speed rotor PMs.

Figures 5, and 6 show the obtained results for the low-speed rotor. Comparing the results of two rotors show that the amplitudes of induced voltages are identical. The total Back EMF is obtained by summing the induced voltages shown in Figure 4 and Figure 6. The total Back EMF depends on the initial positions of two rotors. For a better understanding, the Values of the fundamental component of Back EMF and its THD for various positions of two rotors are presented in Table 3. According to this table, when two rotors are shifted 13 degrees related to each other, the maximum value of Back EMF is achieved. The Back EMF of the machine with 13 degrees shifting angle is shown in Figure 7. As is obvious, the Back EMF waveform is almost sinusoidal.

It should be noted that the machine power angle and rotor positions depend on the output power of each rotor disc. The output power of the machine depends on the values of the armature current and Back EMF. Since the current flows in the coil arms on both sides of the stator is identical, the distributed power between two rotor discs directly depends on the values of induced voltages due to each rotor PMs. It should be noted that the location of each rotor disc affects the amplitude of the Back EMF waveform. Therefore, for simplicity, the machine has been designed in a way that two rotor discs have identical output power and consequently similar Back EMF amplitude, and positions.

Table 1. Machine specifications

Parameter	Value
The output power of each rotor	100 (Watt)
Speed of 14-pole rotor	600 (rpm)
Speed of 10-pole rotor	428 (rpm)
The axial length of the stator core	15 (mm)
The axial length of PMs	5 (mm)
The axial length of the rotor core	7 (mm)
The outer diameter of the machine	220 (mm)
The inner diameter of the machine	113.6 (mm)

Table 2. Materials of the cores, PM, and windings

Parameter	Material
Stator	High silicon–iron alloy
Rotor	Low-carbon steel
PM	NdFeB (N42)
Winding	Copper

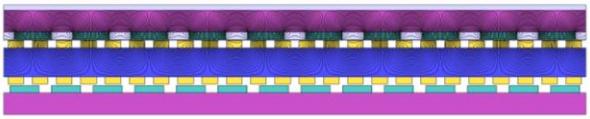

Figure 3. Magnetic Flux path in the machine due to the high-speed rotor PMs.

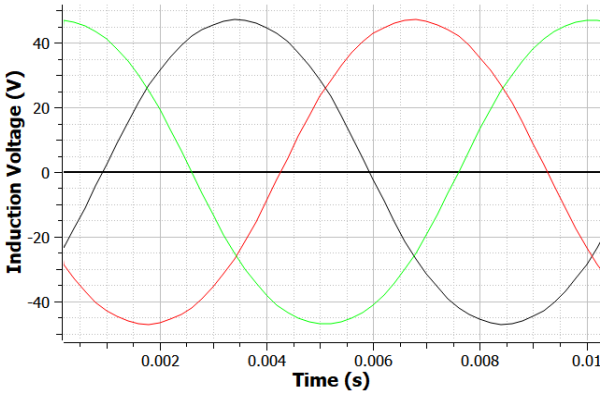

Figure 4. The induced voltage in the armature windings due to the high-speed rotor PMs.

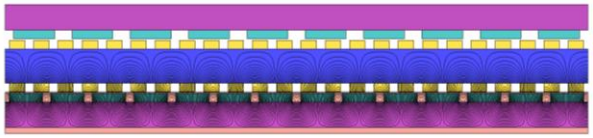

Figure 5. Magnetic Flux path in the machine due to the low-speed rotor PMs.

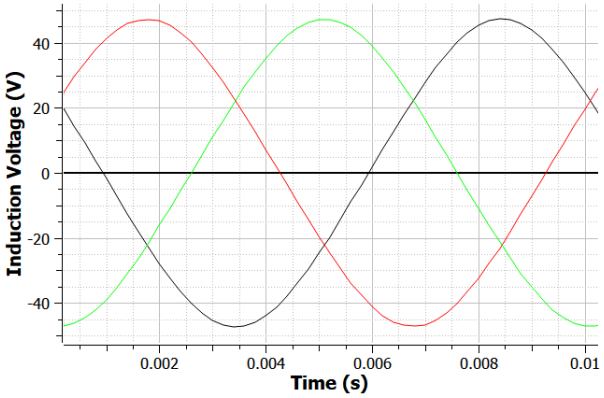

Figure 6. The induced voltage in the armature windings due to the low-speed rotor PMs.

Table 3. The Value of Back EMF for different relative positions of two rotors

The relative position (Degree)	The amplitude of the fundamental component (V)	THD (%)
2.6	31	24
5.2	57	5.43
7.8	77.5	3.17
10.4	90.3	2.27
12	93.7	1.14
13	**94.3**	**0.75**
14.6	92.8	1.71
15.6	89.3	2.44

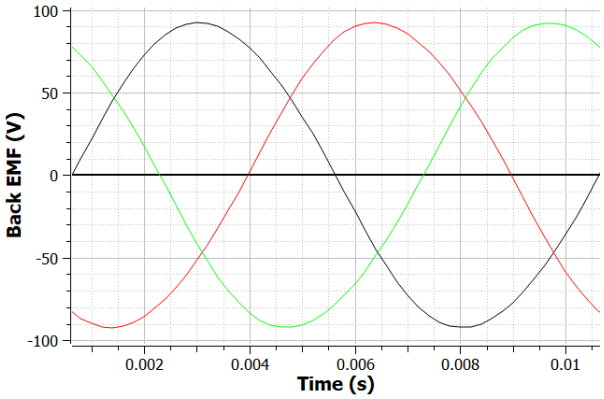

Figure 7. The Back EMF of the machine.

The machine has been tested under full load conditions. For this purpose, a load with a power of 100 watts has been applied to each rotor disc. The three-phase of stator current and input power of the case study machine has been shown in Figure 8 and Figure 9 respectively. The electromagnetic force produced by Stator currents and applied to the low-speed rotor and the high-speed rotor are indicated in Figure 8 and Figure 9. Based on the linear speed and the average radius of the machine, the angular speed of the machine is calculated as:

$$\omega = v / r \tag{1}$$

In which ω, v, and r are the rotor angular speed, linear speed, and average radius, respectively. Also, the output power is obtained as:

$$P_{out} = T\omega = r.F.\omega \tag{2}$$

Where P_{out}, T, and F are the output power, electromagnetic torque, and electromagnetic force, respectively.

By substituting (1) in (2), we have:

$$P_{out} = F.v \tag{3}$$

The linear speed of two rotor discs is shown in Figure 12. With the help of (3) the output power of two rotor discs is calculated. Calculations confirm that the output power of each rotor disc is 100 watts.

By obtaining the output power, the efficiency is calculated as:

$$\eta = \frac{P_{out}}{P_{in}} \tag{4}$$

Where P_{in} is the input power. With the help of (4), the efficiency of the machine would be equal to 78%.

The obtained results confirm that the machine has acceptable performance characteristics.

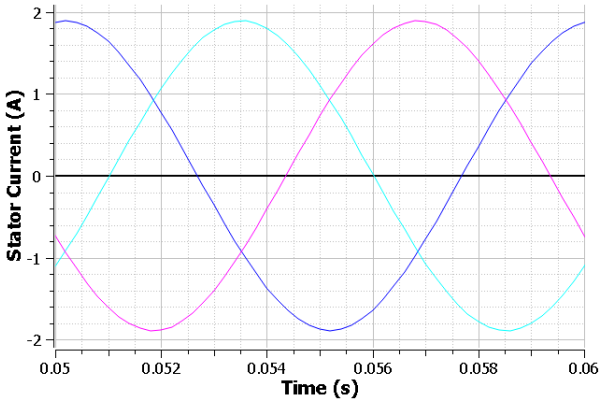

Figure 8. Three-phase of stator current

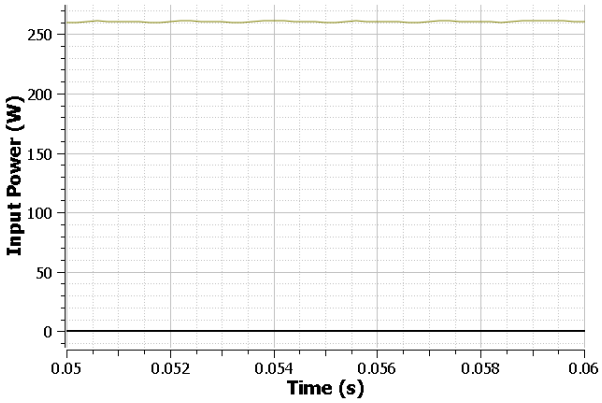

Figure 9. Input power of the machine

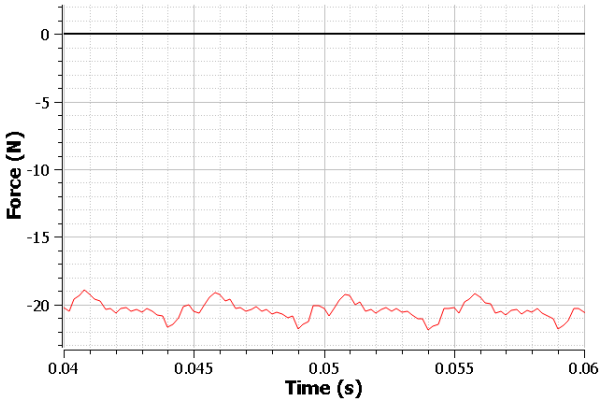

Figure 10. The electromagnetic force applied to the low-speed rotor

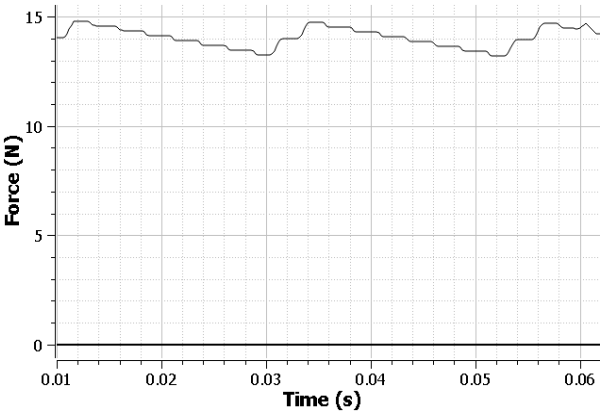

Figure 11. The electromagnetic force applied to the high-speed rotor

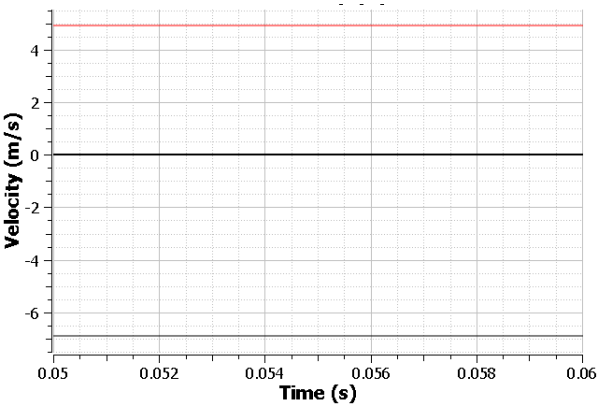

Figure 12. The linear speed of two rotors

Conclusions

In this paper, a new structure of the FSCW-DRAFPMSG has been introduced. The case study machine consists of two permanent magnet rotors with different numbers of poles and different rotating directions. This structure has the ability to rotate in opposite directions at different speeds. The FEM has been used to validate the performance characteristics of the proposed topology. The obtained results show that the machine has a maximum amplitude of Back EMF when two rotor discs are shifted 13 degrees related to each other. In addition, each rotor disc produces 100 watts of power while one rotor rotates at speed of 600 rpm and the other one rotates at speed of 428 rpm. Also, the efficiency of the machine is 78%. This structure is suitable for use in several industrial applications such as gearless elevators or direct-drive ship propulsion systems.

References

[1] Jahns, T.M., 2011. “The expanding role of PM machines in direct-drive applications”. In *2011 International Conference on Electrical Machines and Systems*, August, pp. 1-6.

[2] Piech, J., 2014. “Permanent magnet machines for elevators in super high-rise buildings”. *Council on Tall Buildings and Urban Habitat CTBUH*, p.823.

[3] Cros, J. and Viarouge, P., 2002. “Synthesis of high-performance PM motors with concentrated windings”. *IEEE transactions on energy conversion*, 17(2), pp.248-253.

[4] Magnussen, F. and Sadarangani, C., 2003. “Winding factors and Joule losses of permanent magnet machines with concentrated windings”. In *IEEE International Electric Machines and Drives Conference (IEMDC'03)*, (1), June, pp. 333-339.

[5] Zhu, Z.Q., Azar, Z. and Ombach, G., 2011. “Influence of additional air gaps between stator segments on cogging torque of permanent-magnet machines having modular stators”. *IEEE Transactions on Magnetics*, 48(6), pp.2049-2055.

[6] Valavi, M., Nysveen, A., Nilssen, R., Lorenz, R.D. and Rølvåg, T., 2013. “Influence of pole and slot combinations on magnetic forces and vibration in low-speed PM wind generators”. *IEEE Transactions on Magnetics*, 50(5), pp.1-11.

[7] El-Refaie, A.M., 2009. “Fractional-slot concentrated-windings synchronous permanent magnet machines: Opportunities and challenges”.

IEEE Transactions on Industrial Electronics, 57(1), pp.107-121.

[8] Dajaku, G., Spas, S. and Gerling, D., 2019. "Advanced optimization methods for fractional slot concentrated windings". *Electrical Engineering*, 101(1), pp.103-120.

[9] Yokoi, Y., Higuchi, T. and Miyamoto, Y., 2016. "General formulation of winding factor for fractional-slot concentrated winding design". *IET Electric Power Applications*, 10(4), pp.231-239.

[10] Andrada Gascón, P., Blanqué Molina, B., Martínez Piera, E., Torrent Burgués, M., Sánchez López, J.A. and Perat Benavides, J.I., 2013. "Fractional-slot permanent magnet synchronous generator for low voltage applications". *Electrical Engineering Electronic Journa*l, 1(2).

[11] Kim, B., 2017. "Investigation on slot–pole combinations of a PM vernier motor with fractional-slot concentrated winding configurations". *Energies*, 10(9), p.1310.

[12] Zhao, B., Gong, J., Tong, T., Xu, Y., Semail, E., Nguyen, N.K. and Gillon, F., 2021. "A novel five-phase fractional slot concentrated winding with low space harmonic contents". IEEE Transactions on Magnetics, 57(6), pp.1-5.

[13] Reddy, P.B., El-Refaie, A.M. and Huh, K.K., 2014. "Effect of number of layers on performance of fractional-slot concentrated-windings interior permanent magnet machines". IEEE Transactions on Power Electronics, 30(4), pp.2205-2218.

[14] Gundogdu, T. and Komurgoz, G., 2013. "Implementation of fractional slot concentrated winding technique to large salient-pole synchronous generators & development with permanent magnets". Electric power systems research, 105, pp.57-70.

[15] Taghavi Araghi, S.M., Kiyoumarsi, A. and Mirzaeian Dehkordi, B., 2022. "Synchronous reluctance machines with new type of fractional-slot concentrated-windings based on the concept of stator slot shifting". *IET Electric Power Applications*.